Cell Research (2016) :1-4.

www.nature.com/cr

LETTER TO THE EDITOR

One-step homozygosity in precise gene editing by an improved CRISPR/Cas9 system

Cell Research advance online publication 8 April 2016; doi:10.1038/cr.2016.46

Dear Editor,

The CRISPR/Cas9 gene editing method has been successfully applied to modify genomes in many organisms [1]. However, several critical issues remain unresolved and have become major hurdles for its broad applications [1]. First, editing efficiency varies widely at different genetic loci and some targeted sites are resistant to editing for unknown reasons. Even for the same gene, editing efficiency differs greatly at different positions. Second, generation of undesirable insertions or deletions (InDels) at the target sites constitutes a major issue in precise genome editing and gene therapy. Third, one-step homozygosity in precise gene editing is extremely rare and is highly desirable for genetic and functional analyses, especially in systems where genetic manipulations are not possible or are tedious and time-consuming, such as cultured cells and mammals.

A Cas9-based technique has been established to generate precise nucleotide changes in the *C. elegans* genome using single-stranded oligonucleotides as donor templates [2-8]. In this system, the *eft-3* gene promoter is used to drive Cas9 protein expression in *C. elegans* germline [9, 10]. A SV40 Large T-antigen nuclear localization signal (NLS) is added to the C-terminus of Cas9 to usher it to the nucleus. Precise nucleotide alterations were achieved at multiple target sites with varying efficiencies, but not at some other loci tested [2-7].

To investigate the causes of varying editing efficiencies, we examined the editing efficiency at four different target sites in the *ben-1* gene by screening for *ben-1* loss-of-function mutations, which are dominant suppressors of the Uncoordinated (Unc) phenotype induced by the benomyl drug treatment [2]. We attempted to alter nucleotides at positions 22, 153, 1340 and 1499 of the *ben-1* gene to create a stop codon (Supplementary information, Figure S1A and Data S1). Using a construct, P*eft-3*::Cas9-SV40_NLS::*tbb*-2 3′ UTR [9], which expresses Cas9 with a C-terminal SRAD-NLS tag (named Cas9 I for simplicity; Figure 1A), we only obtained non-Unc F1 progeny from P0 animals injected with the DNA mixture expressing Cas9 I and sgRNA targeting the *ben-1*^{153} position along with the cognate oligonucleotide template (Supplementary information, Figure S1B and Data S1). Approximately 20% of the non-Unc animals contained precise *ben-1*^{153} knock-ins, constituting ~3% of the F1 progeny (Supplementary information, Figure S1B and S1C). Despite multiple attempts, we could not obtain any non-Unc F1 progeny using sgRNAs targeting the *ben-1*^{22}, *ben-1*^{1340} and *ben-1*^{1499} positions (Supplementary information, Figure S1B).

We then tested another Cas9 construct, pDD162 (named Cas9 II) [10], which uses the same *eft-3* promoter to express a Cas9 protein with the identical protein sequence but a slightly different C-terminal tag (Figure 1A). This Cas9 II construct injected at the same concentration in an otherwise identical injection mixture produced non-Unc F1 progeny at all four *ben-1* positions (Supplementary information, Figure S1B). Sequencing analyses confirmed precise editing at all four targeted sites (Supplementary information, Figure S1C-S1F), indicating that Cas9 II has a much better editing ability. Importantly, Cas9 II not only notably enhanced the efficiency of editing at the *ben-1*^{153} position, but also greatly improved the fidelity of editing at this position, from 20% with precise knock-ins among sequenced non-Unc F1 progeny using Cas9 I to 90% with precise knock-ins using Cas9 II (Figure 1B). 70% of Cas9 I-edited animals (38/54) at the *ben-1*^{153} site did not have the designed edit and instead contained InDels, including large InDels (Supplementary information, Figure S1C). By contrast, 90% of Cas9 II-edited animals at the *ben-1*^{153} site contained precise knock-ins and the rest had 1-bp InDels, with 3 also containing the designed edit (Supplementary information, Figure S1C). Altogether, a 20-fold increase in F1 precise editing efficiency was achieved at the *ben-1*^{153} position and precise editing was also obtained at the other three *ben-1* sites with Cas9 II, indicating that Cas9 II is a superior nuclease for gene editing.

The two Cas9 expression constructs have the same promoter, the same Cas9 protein sequence, and the same 3′ UTR sequence, but their Cas9 coding sequences differ in four aspects: codon usage, the intron number, the intron sequence, and the C-terminal tag. In Cas9 I, a

"SRAD" linker sequence is inserted between Cas9 and NLS, whereas in Cas9 II a more flexible "GGSGP" linker is inserted between Cas9 and NLS, with one extra HA tag placed after NLS (Figure 1A). To determine whether one or multiple different elements of these two Cas9 coding sequences affect their editing ability, we generated five additional Cas9 coding sequences (III to VII), with different introns and C-terminal tags (Figure 1A). Gene editing results from using these five new Cas9 constructs along with the same *ben-1*[153] sgRNA and oligonucleotide template indicate that the intron number or sequence does not alter the editing efficiency of Cas9 (Figure 1A

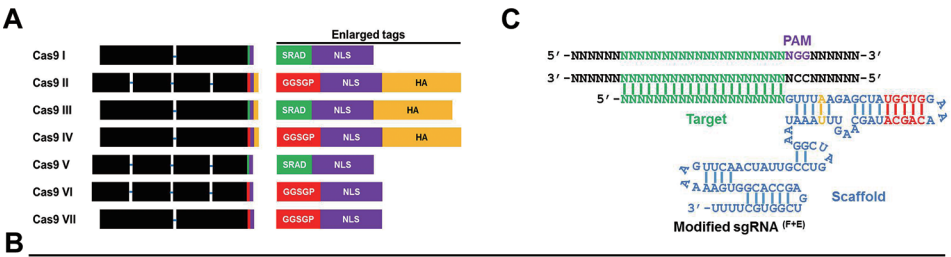

B

editing	Cas9	Benomyl^{R}/F1	Knock-ins/Sequenced	Precise knock-ins/Sequenced	Normalized precise knock-ins/F1	fold
	I	15% (128/848)	30% (16/54)	20% (11/54)	3% (26/848)	1
	II	66% (498/759)	96% (48/50)	90% (45/50)	59% (448/759)	19.7
	III	2% (19/950)	33% (4/12)	33% (4/12)	0.6% (6/950)	0.2
ben-1^{153}	IV	76% (621/822)	79% (15/19)	79% (15/19)	60% (490/822)	20
	V	12% (114/939)	40% (8/20)	35% (7/20)	4% (40/939)	1.3
	VI	41% (425/1031)	88%(23/26)	81%(21/26)	33% (343/1031)	11
	VII	54% (512/957)	83%(24/29)	83%(24/29)	44% (423/957)	14.7

D

Editing site	Cas9	Cas9 I		Cas9 II	
	sgRNA	sgRNA	sgRNA $^{(F+E)}$	sgRNA	sgRNA $^{(F+E)}$
ben-1^{22}	Benomyl^{R}/ F1	0% (0/865)	0% (0/997)	0.8% (5/625)	26% (214/810)
	Precise knock-ins/Sequenced	NA	NA	80% (4/5)	68% (15/22)
drp-1^{D118A}	Knock-ins/Benomyl^{R} F1	0% (0/192)	0% (0/192)	27% (51/192)	50% (96/192)
	Precise knock-ins/Sequenced	NA	NA	100% (14/14)	100% (21/21)
flag::ced-9	Knock-ins/Benomyl^{R} F1	0% (0/192)	0% (0/192)	0% (0/384)	6% (11/192)
	Precise knock-ins/Sequenced	NA	NA	NA	73% (8/11)

E

Editing site	Cas9 and sgRNA	Knock-ins/Benomyl^{R} F1	Homozygous knock-ins/Benomyl^{R} F1	Precise homozygous knock-ins/Benomyl^{R} F1
drp-1^{D118A}	Cas9 I and sgRNA	0% (0/192)	0% (0/192)	0% (0/192)
	Cas9 II and sgRNA	27% (51/192)	0% (0/192)	0% (0/192)
	Cas9 II and sgRNA$^{(F+E)}$	50% (96/192)	3% (6/192)	3% (6/192)
fis-2$^{N49L/K50ochre}$	Cas9 I and sgRNA	2% (4/192)	0% (0/192)	0% (0/192)
	Cas9 II and sgRNA	20% (19/96)	2% (2/96)	2% (2/96)
	Cas9 II and sgRNA$^{(F+E)}$	36% (35/96)	6% (6/96)	6% (6/96)
ubr-1^{M80ochre}	Cas9 I and sgRNA	3% (5/192)	0% (0/192)	0% (0/192)
	Cas9 II and sgRNA	30% (29/96)	0% (0/96)	0% (0/96)
	Cas9 II and sgRNA$^{(F+E)}$	54% (52/96)	9% (9/96)	7% (7/96)

Figure 1 A new combination of Cas9 and sgRNA greatly improves editing efficiency and fidelity and drives one-step homozygosity. **(A)** A schematic diagram of Cas9 proteins with different C-terminal tags. The black boxes depict the exons of the Cas9 coding region and the blue lines depict the introns. **(B)** The editing efficiencies at the *ben-1*[153] position mediated by seven different Cas9 proteins shown in **A**. The normalized percentage of precise knock-ins identified from the total F1 animals screened is also shown. **(C)** A diagram of sgRNA$^{(F+E)}$ and its target DNA. The sequences shared by regular sgRNA and sgRNA$^{(F+E)}$ are in blue. An A-U base-pair flip and an extension of the first stem-loop in the scaffold of sgRNA$^{(F+E)}$ are highlighted in yellow and red, respectively. **(D)** Editing efficiencies of different combinations of Cas9 I or Cas9 II with regular sgRNA or sgRNA$^{(F+E)}$ at the indicated positions. For editing experiments at the *ben-1*[22] position, editing results were scored and presented as in **B**. For editing experiments at the *drp-1*[118] position and the *ced-9* locus, a co-CRISPR method, which includes a driver sgRNA proven to work well in editing, was used to facilitate the identification of edited F1 animals [3, 4]. The *ben-1*[153] sgRNA was used as a co-CRISPR driver. **(E)** Comparison of the editing efficiencies in generating F1 homozygotes with the indicated editings using different combinations of Cas9 I or Cas9 II with sgRNA or sgRNA$^{(F+E)}$. The co-CRISPR method was used to enrich F1 edited animals, as in **D**.

and 1B). The C-terminal tags to Cas9 do have a profound effect on both its editing efficiency and accuracy (Figure 1B and Supplementary information, Figure S1G). For example, Cas9 II and Cas9 IV with the same C-terminal tag showed 66% and 76% editing efficiency (Benomyl^{R}/F1), respectively, which is 4-5-fold higher than those of Cas9 I and Cas9 V with a Cas9 I C-terminal tag (Figure 1B). Importantly, Cas9 II and Cas9 IV showed high editing fidelity (90% and 79% precise knock-ins/sequenced Benomyl^{R} F1, respectively), whereas Cas9 I and Cas9 V showed only 20% and 35% editing accuracy, respectively (Figure 1B and Supplementary information, Figure S1C and S1G). Interestingly, removal of the HA motif from the Cas9 II C-terminal tag reduced the editing efficiency of the two resulting Cas9 variants, but not their editing fidelity (Cas9 VI and VII; Figure 1A and 1B), whereas addition of the HA motif to the Cas9 I C-terminal tag markedly decreased the editing efficiency of the resulting Cas9 protein (Cas9 III, Figure 1A and 1B). These results indicate that the C-terminal tag attached to Cas9 unexpectedly plays a critical role in determining both the editing efficiency and accuracy of Cas9 and that a flexible GGSGP linker between NLS and Cas9 is important for robust and accurate editing.

We then examined whether placement of an NLS at the N-terminus of Cas9 also affects its editing ability. An NLS immediately before Cas9 II (Cas9 VIII) drastically reduced its editing efficiency (from 66% to 4%) at the *ben-1*^{153} position (Supplementary information, Figure S1H-S1J). Addition of an NLS immediately before Cas9 (Cas9 IX), which has no tag at its C-terminus, resulted in an even worse editing efficiency (Supplementary information, Figure S1H-S1J). Insertion of a flexible linker, GGSGP, or its reversed version (PGSGG), between NLS and Cas9 in Cas9 VIII, marginally improved the editing efficiency of the two resulting Cas9 proteins (Cas9 X and Cas9 XI) over Cas9 VIII (Supplementary information, Figure S1H-S1J). Together, these results indicate that an N-terminal NLS tag to Cas9, even with a flexible linker, is detrimental to Cas9 activity.

A structurally optimized sgRNA, sgRNA$^{(F+E)}$, was designed to improve imaging of genomic loci in cells by a GFP-tagged, nuclease-defective Cas9 protein [11]. Two modifications are made in sgRNA$^{(F+E)}$, in which "F" is an A-U base pair flip that destroys a potential polymerase III terminator (UUUU) and "E" is a 5-bp extension of the Cas9-binding hairpin structure that likely improves the assembly of the sgRNA/Cas9 complex (Figure 1C). We tested whether sgRNA$^{(F+E)}$ improves gene editing at two different loci, the *ben-1*^{22} position and the *drp-1*^{118} position (Figure 1D). Editing at these two sites was unsuccessful using Cas9 I and occurred at a low-to-moderate frequency using Cas9 II (Figure 1D). sgRNA$^{(F+E)}$, when used with Cas9 I, did not produce successful editing at either target site. By contrast, using sgRNA$^{(F+E)}$ with Cas9 II led to a 32-fold increase in editing efficiency at the *ben-1*^{22} position and a 1.8-fold increase at the *drp-1*^{118} position compared with the sgRNA/Cas9 II combination (Figure 1D and Supplementary information, Figure S2A and S2B). Moreover, using sgRNA$^{(F+E)}$/Cas9 II, we precisely inserted a 24-bp FLAG-coding sequence right after the initiation codon of the *ced-9* gene at a reasonable frequency (4%), which was not achieved in our multiple attempts using the sgRNA/Cas9 I, sgRNA/Cas9 II, or sgRNA$^{(F+E)}$/Cas9 I combination (Figure 1D and Supplementary information, Figure S2C). We could also precisely insert a large tag, such as GFP, at targeted loci using sgRNA$^{(F+E)}$/Cas9 II and circular DNA templates with varying efficiencies (data not shown). Therefore, sgRNA$^{(F+E)}$ has the ability to greatly enhance the efficiency of precise editing when combined with Cas9 II.

Remarkably, the sgRNA$^{(F+E)}$/Cas9 II combination also produced a low but significant frequency (3%) of the *drp-1*^{D118A} homozygous mutants in F1 progeny of the injected animals, wherein both chromosomes of the F1 animals were precisely edited (Figure 1E and Supplementary information, Figure S2D). This one-step homozygosity in template-mediated precise gene editing is very rare and thought to be extremely difficult to achieve [3, 4]. It occurs rarely in other systems [1] and is highly desirable in experimental systems not amenable to genetic manipulations.

We tested whether sgRNA$^{(F+E)}$/Cas9 II can generate precisely edited homozygous F1 mutants at two other loci, the *fis-2* and *ubr-1* genes (Figure 1E) and were able to obtain a reasonable frequency (6%-7%) of precise F1 homozygous mutants (Figure 1E, Supplementary information, Figure S2E and S2F). As we failed to obtain F1 homozygous *drp-1*^{D118A} and *ubr-1*^{M80ochre} mutants using sgRNA/Cas9 II, despite getting substantial percentages of F1 heterozygous *drp-1*^{D118A} and *ubr-1*^{M80ochre} mutants (Figure 1E), sgRNA$^{(F+E)}$, which works in multiple organisms [11], appears to be a key driver for one-step homozygosity in gene editing. This unique sgRNA$^{(F+E)}$/Cas9 II combination should enable generation of homozygous F1 mutants at most genetic loci in *C. elegans* and may be applicable to other experimental systems.

We last used database analysis and molecular dynamics (MD) simulation to investigate how different C-terminal tags affect the editing efficiency of Cas9. Both analyses suggest that the GGSGP linker is flexible and capable of adopting various conformations, while the SRAD linker is more rigid and tends to take a locally bent structure due to a stable electrostatic interaction between its Arg residue and Asp residue (Supplementary information, Figure S2G, S2H and Data S1). Since all

Cas9 crystal structures lack a C-terminal tag [12-14], we modeled the structures of Cas9 I and Cas9 II by taking the representative conformations of SRAD and GGSGP from simulation trajectories and the structures of NLS and HA from structural databases (Supplementary information, Figure S2G, S2H and Data S1). In the modeled structures, the structurally flexible GGSGP linker allows the highly positively charged NLS sequence in Cas9 II to interact favorably with negatively charged nucleic acids (Supplementary information, Figure S2I), which likely reinforces the interaction between Cas9 and DNA or/and sgRNA and thus enhances the cleavage activity and specificity of Cas9 [12-14] (Figure 1B). By contrast, the shorter and locally bent SRAD linker in Cas9 I does not provide sufficient flexibility to facilitate the interaction between the NLS tag and nucleic acids (Supplementary information, Figure S2J). Moreover, the HA sequence at the C-terminus of Cas9 II may further stabilize the formation of the Cas9/sgRNA/DNA ternary complex, resulting in further increase of the Cas9 activity (Figure 1B and Supplementary information, Figure S2I). Interestingly, a Pro-to-Ala substitution (Cas9 XII) along with substitutions of two negatively charged Asp residues in the HA tag of Cas9 II with two positively charged Lys residues (Cas9 XIII) or two neutral Ala residues (Cas9 XIV) to generate a more flexible HA tag markedly reduce rather than enhance the editing efficiency of Cas9 (Supplementary information, Figure S2K-S2M). These findings, and the observations that addition of the HA tag to Cas9 I and removal of the HA tag from Cas9 II and Cas9 IV both compromise the editing efficiency (Figure 1A and 1B), indicate that a C-terminal HA tag also has an important impact on the editing efficiency of Cas9.

The ability to alter at will any site in the genome with high fidelity is the ultimate goal of genome engineering. Multiple studies have reported improved CRISPR/Cas9 systems that significantly increase the efficiency of precise gene editing in *C. elegans* through improved screening methods [3, 4, 15], modification of sgRNAs [6, 7], inactivation of genes involved in non-homologous end joining [6], and direct injection of *in vitro* assembled Cas9/sgRNA ribonucleoprotein complexes [8]. In this study, we report a Cas9/sgRNA combination that greatly improves the editing efficiency and fidelity and enables precise editing at all genetic loci tested in *C. elegans*. Importantly, this robust system also permits one-step generation of precise homozygous mutations at multiple tested target sites with a reasonable success rate, which has not been achieved before. This important technical advance will greatly facilitate genetic and functional analysis in *C. elegans*, for instance, by allowing effortless construction of double or triple mutations on closely linked genes and facile assembly of homozygous mutants on multiple genes of interest. Surprisingly, the N-terminal or C-terminal addition of short polypeptide sequences to Cas9 has a profound effect on its editing efficacy and fidelity. This finding suggests the possibility of further improvement of the Cas9 editing efficiency and fidelity in *C. elegans* and other systems through altering or substituting N-terminal or C-terminal tags or sequences.

Acknowledgments

We thank GS Ou for providing plasmids. This work was supported by the National Basic Research Program of China (973 program; 2013CB945600), the National High-Tech R&D Program of China (2013ZX10002-002), a Postdoctoral Science Foundation Grant (2015M570078 to PZ), a Tsinghua-Peking University Life Science Center postdoctoral fellowship (to PZ), and US National Institutes of Health (NIH; R01 GM59083 and R01 GM79097 and R35 GM118188 to DX).

Pei Zhao[1, 2, *], Zhe Zhang[1, *], Xiaoying Lv[3], Xiang Zhao[1], Yuji Suehiro[4], Yinan Jiang[3], Xinquan Wang[3], Shohei Mitani[4], Haipeng Gong[3], Ding Xue[1, 5]

[1]School of Life Sciences & Collaborative Innovation Center for Diagnosis and Treatment of Infectious Diseases, Tsinghua University, Beijing 100084, China; [2]Tsinghua University-Peking University Joint Center for Life Science, Beijing 100084, China; [3]School of Life Sciences, Tsinghua University, Beijing 100084, China; [4]Department of Physiology, Tokyo Women's Medical University, School of Medicine, and Core Research for Evolutional Science and Technology (CREST), Japan Science and Technology Agency, Tokyo 162-8666, Japan; [5]Department of Molecular, Cellular, and Developmental Biology, University of Colorado, Boulder, CO 80309, USA

*These two authors contributed equally to this work.
Correspondence: Ding Xue
E-mail: ding.xue@colorado.edu

References

1 Doudna JA, Charpentier E. *Science* 2014; **346**:1258096.
2 Zhao P, Zhang Z, Ke H, Yue Y, Xue D. *Cell Res* 2014; **24**:247-250.
3 Kim H, Ishidate T, Ghanta KS, *et al*. *Genetics* 2014; **197**:1069-1080.
4 Arribere JA, Bell RT, Fu BX, *et al*. *Genetics* 2014; **198**:837-846.
5 Paix A, Wang Y, Smith HE, *et al*. *Genetics* 2014; **198**:1347-1356.
6 Ward JD. *Genetics* 2015; **199**:363-377.
7 Farboud B, Meyer BJ. *Genetics* 2015; **199**:959-971.
8 Paix A, Folkmann A, Rasoloson D, Seydoux G. *Genetics* 2015; **201**:47-54.
9 Friedland AE, Tzur YB, Esvelt KM, *et al*. *Nat Methods* 2013; **10**:741-743.
10 Dickinson DJ, Ward JD, Reiner DJ, Goldstein B. *Nat Methods* 2013; **10**:1028-1034.
11 Chen B, Gilbert LA, Cimini BA, *et al*. *Cell* 2013; **155**:1479-1491.
12 Jinek M, Jiang F, Taylor DW, *et al*. *Science* 2014; **343**:1247997.
13 Nishimasu H, Ran FA, Hsu PD, *et al*. *Cell* 2014; **156**:935-949.
14 Anders C, Niewoehner O, Duerst A, Jinek M. *Nature* 2014; **513**:569-573.
15 Dickinson DJ, Pani AM, Heppert JK, Higgins CD, Goldstein B. *Genetics* 2015; **200**:1035-1049.

(**Supplementary information** is linked to the online version of the paper on the *Cell Research* website.)

A

B

	Cas9	Benomyl^R/F1	Knock-ins/Sequenced	Precise knock-ins/Sequenced	Normalized precise knock-ins/F1
ben-1^{22}	I	0% (0/865)	NA	NA	0% (0/865)
	II	0.8% (5/625)	80% (4/5)	80% (4/5)	0.6% (4/625)
ben-1^{153}	I	15% (128/848)	30% (16/54)	20% (11/54)	3% (26/848)
	II	66% (498/759)	96% (48/50)	90% (45/50)	59% (448/759)
ben-1^{1340}	I	0% (0/894)	NA	NA	0% (0/894)
	II	3% (24/802)	88% (21/24)	71% (17/24)	2% (17/802)
ben-1^{1499}	I	0% (0/855)	NA	NA	0% (855)
	II	25% (211/843)	100% (13/13)	92% (12/13)	23% (195/843)

Supplementary information, Figure S1 Cas9 proteins with different C-terminal tags display dramatically different editing efficiencies. **(A)** Sequences of different *ben-1* sgRNA target sites and corresponding oligonucleotide repair templates used in the editing experiments. The protospacer adjacent motif (PAM) sequences are highlighted with purple and the sequences targeted by sgRNAs are underlined. The nucleotide altered in each targeted site is indicated in red. The codons of the modified amino acids are marked by a dash on the top. The oligonucloeotide templates used to edit the *ben-1*^{1340} position and the *ben-1*^{1499} position are reverse complement to the sequences of the oligonucloeotides shown. The numbers in parentheses indicate the lengths of homology arms not shown in the repair templates. **(B)** Comparison of the editing efficiencies by Cas9 I and Cas9 II at the *ben-1*^{22}, *ben-1*^{153}, *ben-1*^{1340} and *ben-1*^{1499} positions, respectively. NA, not applicable. The number of benomyl-resistant F1 animals identified from the number of total F1 animals screened (benomyl^R/F1), the number of knock-ins from the number of benomyl^R F1 animals sequenced (Knock-ins/Sequenced), and the number of precise knock-ins from the number of benomyl^R F1 animals sequenced (Precise knock-ins/Sequenced) are shown, respectively. The normalized percentage of precise knock-ins identified from the total number of F1 animals screened (Normalized precise knock-ins/F1) is also shown. For each experiment, 5-7 wild-type N2 animals were injected.

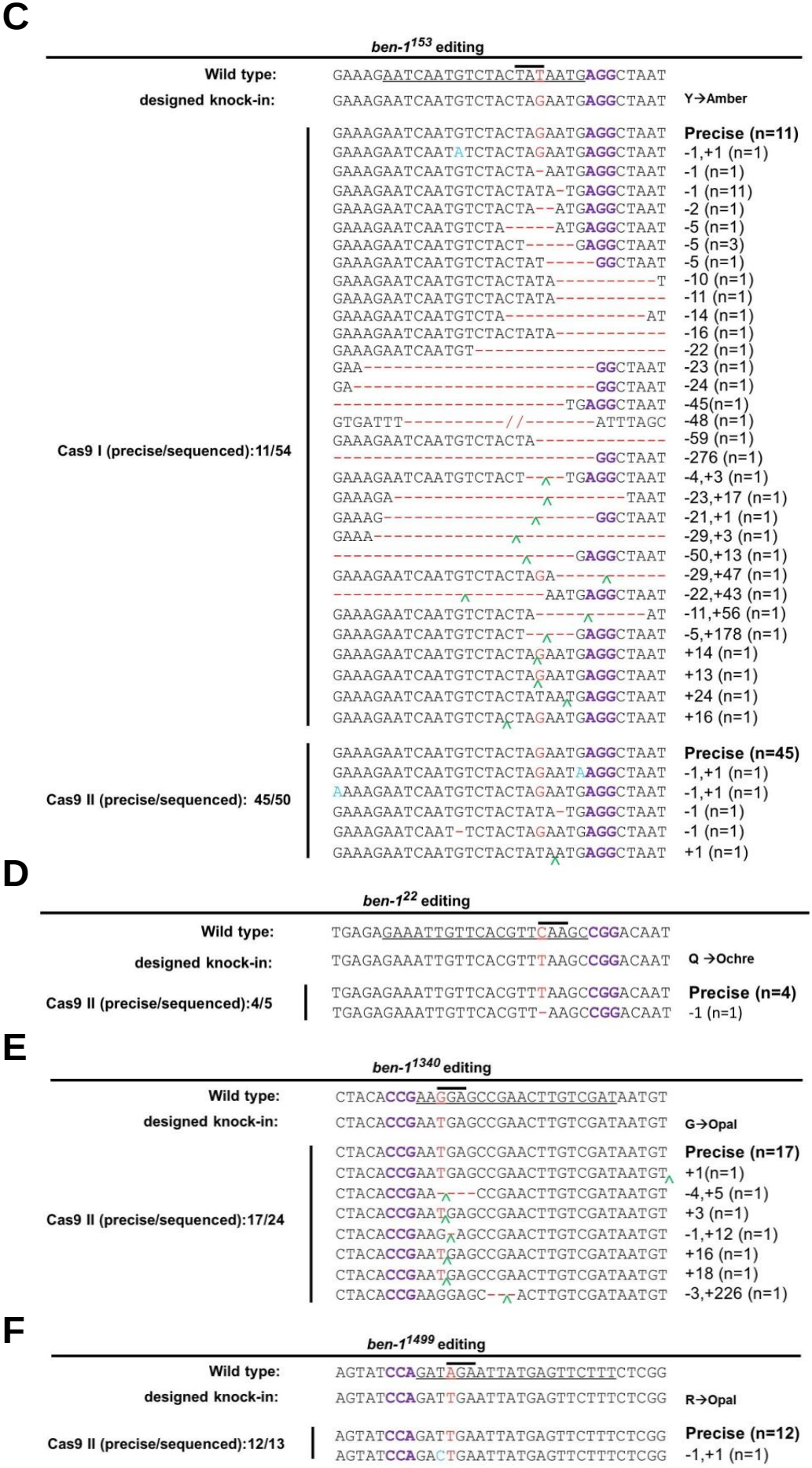

Supplementary information, Figure S1 Cas9 proteins with different C-terminal tags display dramatically different editing efficiencies. **(C-F)** Sequences of wild type animals and Cas9-edited (Cas9 I or Cas9 II) animals around the *ben-1*^{153} **(C)**, *ben-1*^{22} **(D)**, *ben-1*^{1340} **(E)**, and *ben-1*^{1499} **(F)** positions are shown. The protospacer adjacent motif (PAM) sequences are highlighted in purple and the sequences targeted by sgRNAs are underlined. The nucleotide altered at each target site is indicated in red. The codon for the modified amino acid is marked by a dash on the top. The red dashes (-) depict the deleted nucleotides. The green insertion marker (∧) indicates the position of the inserted nucleotides or sequences. The double slashes (//) indicate that there is a long DNA sequence not shown. The replaced nucleotides are highlighted in blue and indicated as “-1 +1”. The numbers of deleted (-n) or/and inserted (+n) nucleotides are listed to the right of each sequence. The number in the parenthesis indicates the number of independently edited animals with the edited sequence shown on the left.

G

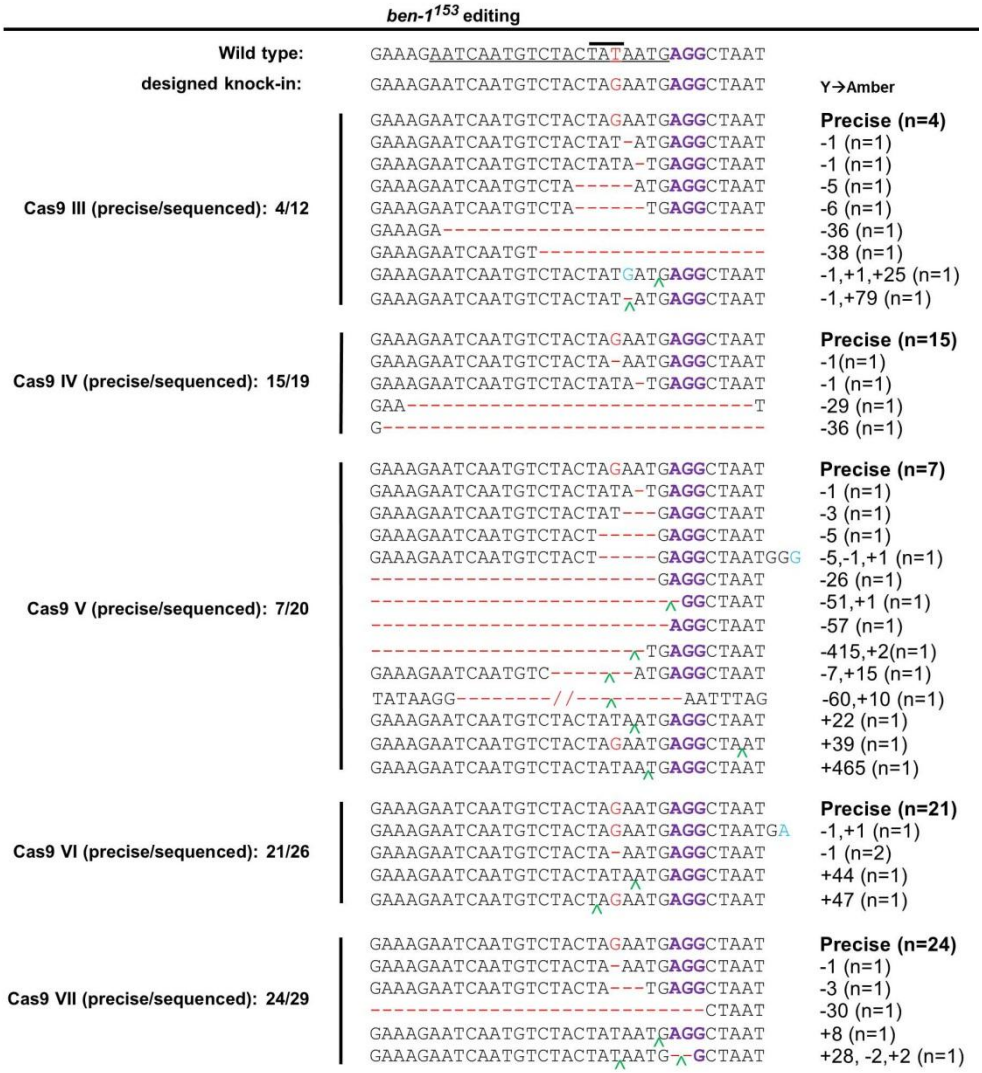

Supplementary information, Figure S1 Cas9 proteins with different C-terminal tags display dramatically different editing efficiencies. **(G)** Sequences of wild type animals and different Cas9-edited animals around the *ben-1*[153] position. Sequences of wild type animals and different Cas9-edited (Cas9 III, Cas9 IV, Cas9 V, Cas9 VI and Cas9 VII) animals around the *ben-1*[153] position are shown. Sequences of Cas9 I- and Cas9 II-edited animals around the *ben-1*[153] position are presented in Supplementary information, Figure S1C. The protospacer adjacent motif (PAM) sequences are highlighted in purple and the sequences targeted by sgRNAs are underlined. The nucleotide altered at each target site is indicated in red. The codon for the modified amino acid is marked by a dash on the top. The red dashes (-) depict the deleted nucleotides. The green insertion marker (∧) indicates the position of the inserted nucleotides or sequence. The double slashes (//) indicate that there is a long DNA sequence not shown. The replaced nucleotides are highlighted in blue and indicated as "-1 +1". The numbers of deleted (-n) or/and inserted (+n) nucleotides are listed to the right of each sequence. The number in the parenthesis indicates the number of independently edited animals with the edited sequence shown on the left.

H

I

	Cas9	Benomyl^{R}/F1	Knock-ins/Sequenced	Precise knock-ins/Sequenced	Normalized precise knock-ins/F1
	II	66% (498/759)	96% (48/50)	90% (45/50)	59% (448/759)
	VIII	4% (43/1156)	90% (18/20)	85% (17/20)	3% (37/1156)
***ben-1*^{153}**	IX	0.3% (3/1092)	100% (2/2)	50% (1/2)	0.1% (1/1092)
	X	12% (133/1156)	82% (14/17)	71% (12/17)	8% (94/1156)
	XI	6% (72/1116)	67% (6/9)	56% (5/9)	4% (40/1116)

J

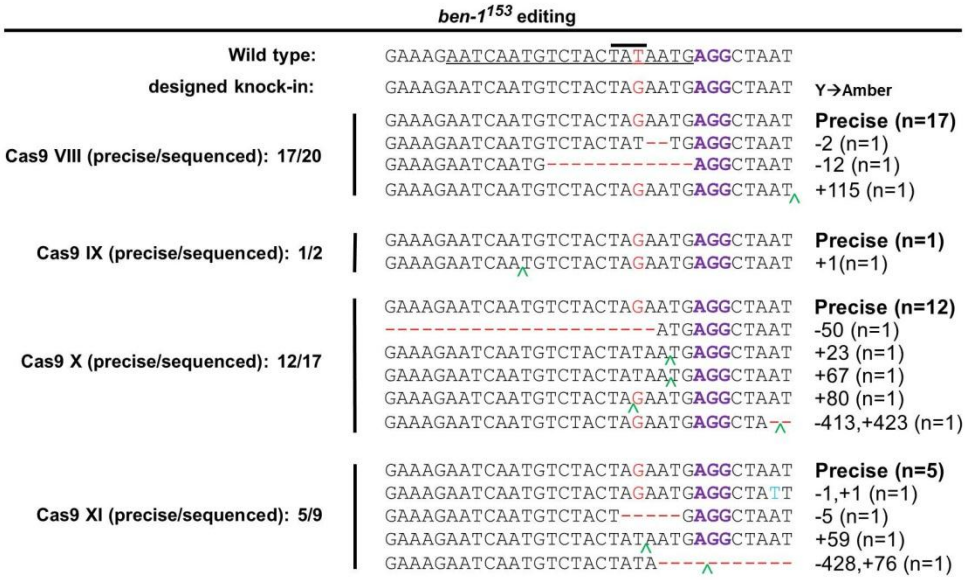

Supplementary information, Figure S1 Cas9 proteins with different C-terminal tags display dramatically different editing efficiencies. **(H)** A schematic diagram of Cas9 proteins with different N-terminal and C-terminal tags. The black boxes depict Cas9-coding exons and the blue lines depict the introns. The red boxes depict the GGSGP linker, the purple boxes depict SV40 NLS, the yellow boxes depict the HA tag, and the blue box depicts the PGSGG linker. **(I)** Comparison of the gene editing efficiencies at the *ben-1*^{153} position by five different Cas9 proteins shown in H. The number of benomyl-resistant (benomyl^{R}) F1 animals identified from the number of total F1 animals screened, the number of knock-ins from the number of benomyl^{R} F1 animals sequenced, and the number of precise knock-ins from the number of benomyl^{R} F1 animals sequenced are shown, respectively**.** The normalized percentage of precise knock-ins identified from the total number of F1 animals screened is also shown. For each experiment, 5-7 wild-type N2 animals were injected. **(J)** Sequences of wild type animals and different Cas9-edited (Cas9 VIII, Cas9 IX, Cas9 X and Cas9 XI) animals around the *ben-1*^{153} position are shown as described in Supplementary information, Figure S1C.

K

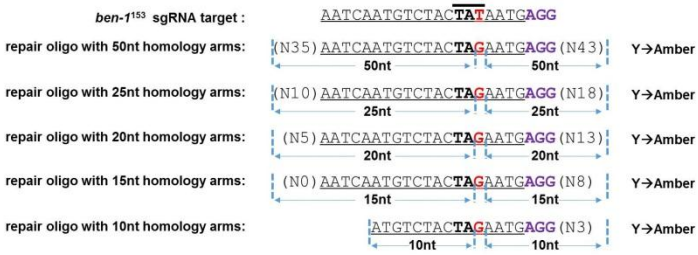

L

	Length of homology arms	10nt	15nt	20nt	25nt	50nt
ben-1^{153}	**Knock-ins/sequenced**	14% (3/21)	20% (5/25)	79% (19/24)	92% (22/24)	96% (48/50)
	Precise knock-ins/sequenced	14% (3/21)	20% (5/25)	79% (19/24)	92% (22/24)	90% (45/50)

Supplementary information, Figure S1 Cas9 proteins with different C-terminal tags display dramatically different editing efficiencies. **(K)** Sequences of the *ben-1*^{153} sgRNA target site and five different oligonucleotide repair templates used in the editing experiments, which contain 50nt, 25nt, 20nt, 15nt and 10nt homology arms, respectively, as described in Figure S1A. The lengths of homology arms in each oligonucleotide are indicated. **(L)** Comparison of the editing efficiencies at the *ben-1*^{153} position when different lengths of oligonucleotide repair templates are used. The number of knock-ins from the number of benomyl-resistant F1 (benomyl^{R} F1) animals sequenced (Knock-ins/Sequenced) and the number of precise knock-ins from the number of benomyl^{R} F1 animals sequenced (Precise knock-ins/Sequenced) are shown. For each experiment, 5-7 wild-type N2 animals were injected.

M

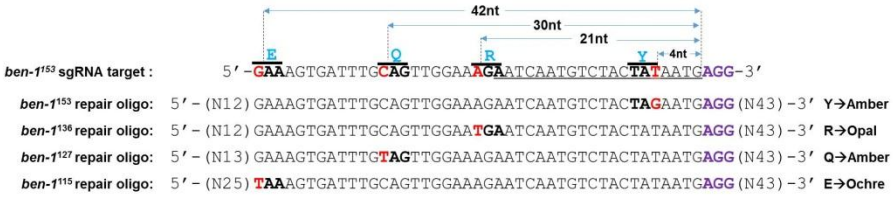

N

Editing	*ben*-1^{153}	*ben*-1^{136}	*ben*-1^{127}	*ben*-1^{115}
Distance between PAM and the knock-in site	4nt	21nt	30nt	42nt
Knock-ins/Sequenced	96% (48/50)	71% (15/21)	33% (7/21)	10% (2/20)
Precise knock-ins/Sequenced	90% (45/50)	52% (11/21)	14% (3/21)	10% (2/20)

Supplementary information, Figure S1 Cas9 proteins with different C-terminal tags display dramatically different editing efficiencies. **(M)** Sequences of the *ben-1*^{153} sgRNA target site and oligonucleotide repair templates used to create stop codons at four different *ben-1* positions. The PAM sequence is highlighted with purple and the sequence targeted by the sgRNA is underlined. The nucleotide altered in each knock-in site is indicated in red. The codons for the modified amino acids are marked by a dash on the top and the amino acids altered shown in blue and listed on the top of the dash. The numbers in parentheses indicate the lengths of homology arms not shown in the repair templates. The distance between the PAM sequence and the nucleotide altered is indicated by a pair of blue arrows. **(N)** Comparison of the editing efficiencies of Cas9 II at four different *ben-1* sites, *ben-1*^{153}, *ben-1*^{136}, *ben-1*^{127} and *ben-1*^{115}, respectively. The same *ben-1*^{153} sgRNA was used in these editing experiments. The distance between the PAM sequence and the nucleotide altered, the number of knock-ins from the number of benomyl-resistant F1 (benomyl^{R} F1) animals sequenced (Knock-ins/Sequenced), and the number of precise knock-ins from the number of benomyl^{R} F1 animals sequenced (Precise knock-ins/Sequenced) are shown, respectively. For each experiment, 5-7 wild-type N2 animals were injected.

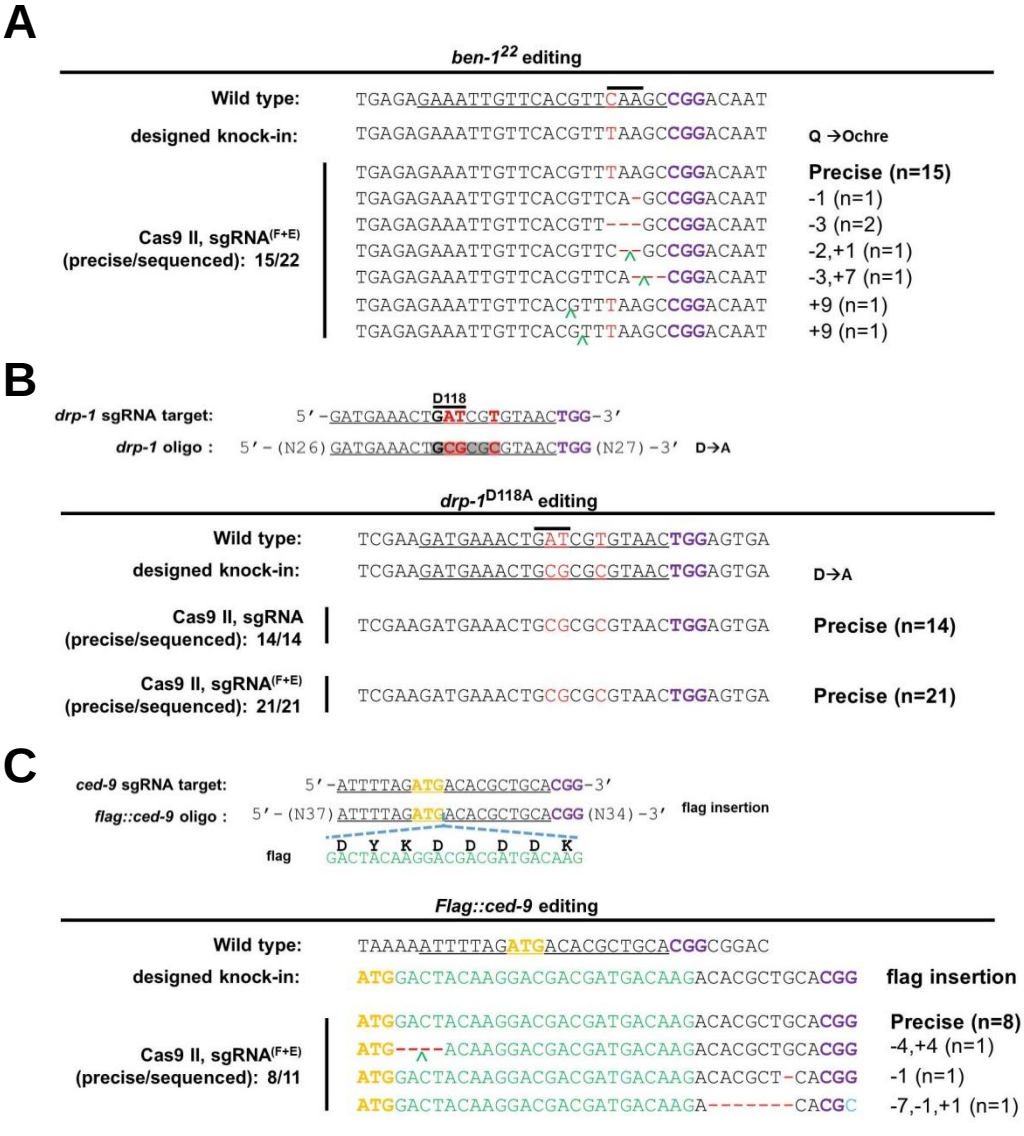

Supplementary information, Figure S2 A structurally optimized sgRNA$^{(F+E)}$ enhances the editing efficiency of Cas9 II and structural modeling of Cas9 I and Cas9 II. **(A-C)** Sequences of wild type animals and different Cas9-edited animals (mediated by different combinations of Cas9 I or Cas9 II with regular sgRNA or sgRNA$^{(F+E)}$) around the *ben-1*^{22} **(A)**, the *drp-1*^{D118A} **(B)**, and the *ced-9* **(C)** sgRNA target sites are shown. Sequences of Cas9 II/sgRNA-edited animals around the *ben-1*^{22} position are shown in supplementary information, Figure S1D. Sequences of sgRNA target sites and oligonucleotide templates used in *drp-1*^{D118A} and *ced-9* editing experiments are shown above the corresponding sequencing results and presented as in Supplementary information, Figure S1A. The protospacer adjacent motif (PAM) sequences are highlighted in purple and the sequences targeted by sgRNAs are underlined. The nucleotides altered at each target site are indicated in red. The codon for the modified amino acid is marked by a dash on the top **(A, B).** To generate a BssH II restriction site (marked with a gray box) at the *drp-1*^{D118A} position, a silent mutation was introduced at residue Arg119 (CGT to CGC). The translation initiation codon of *ced-9* is highlighted in yellow and the Flag-coding sequence inserted after the initiation codon is highlighted in green **(C)**. The red dashes (-) depict the deleted nucleotides. The green insertion marker (^**)** indicates the position of the inserted nucleotides. The replaced nucleotides are highlighted in blue and indicated as “-1 +1”. The numbers of deleted (-n) or/and inserted (+n) nucleotides are listed to the right of each sequence. The number in the parenthesis indicates the number of independently edited animals with the edited sequence shown on the left.

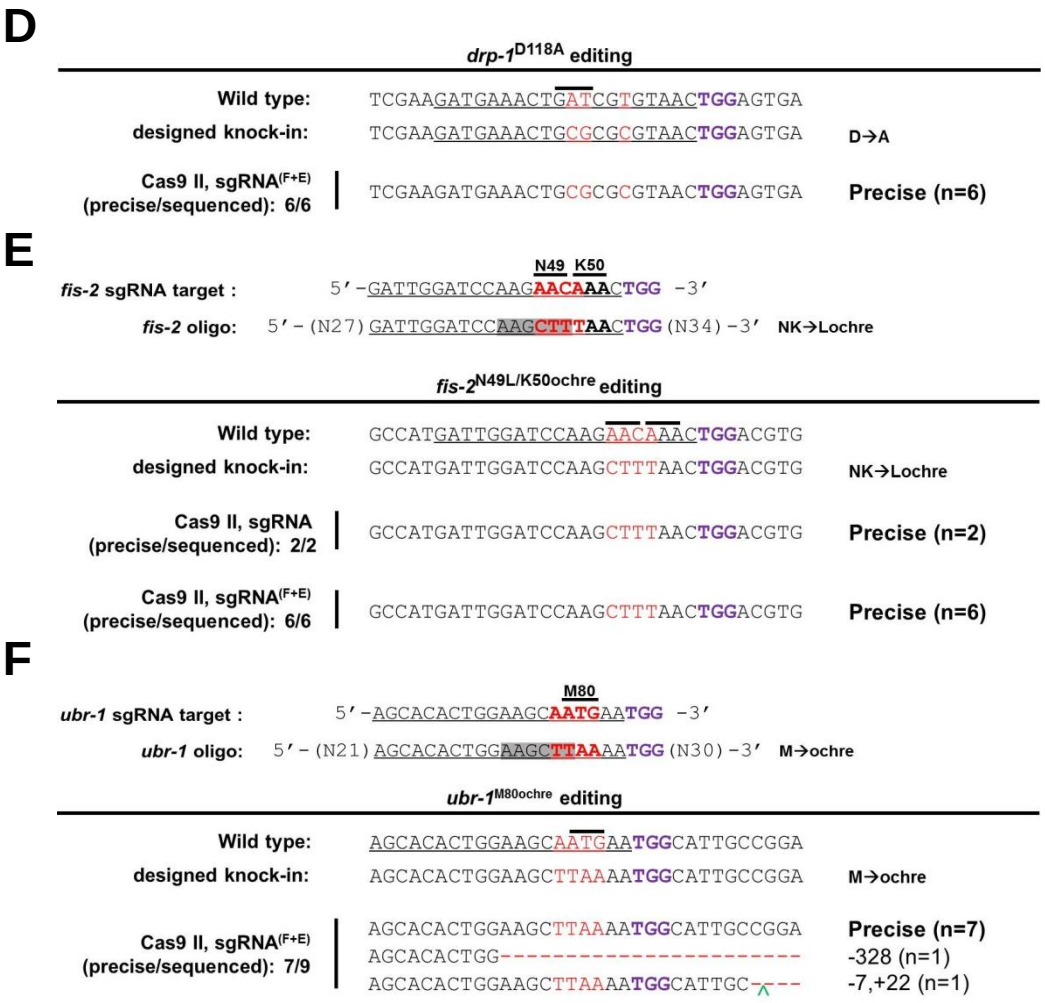

Supplementary information, Figure S2 A structurally optimized sgRNA$^{(F+E)}$ enhances the editing efficiency of Cas9 II and structural modeling of Cas9 I and Cas9 II. **(D-F)** Sequences of wild type animals and different Cas9-edited F1 homozygous animals (mediated by different combinations of Cas9 I or Cas9 II with regular sgRNA or sgRNA$^{(F+E)}$) around the *drp-1*^{D118A} **(D)**, the *fis-2*$^{N49L/K50ochre}$ **(E)**, and the *ubr-1* ^{M80ochre} **(F)** sgRNA target sites are shown. Sequences of sgRNA target sites and oligonucleotide repair templates used in the *fis-2*$^{N49L/K50ochre}$ and *ubr-1* ^{M80ochre} editing experiments are shown above the corresponding sequencing results and presented as in Supplementary information, Figure S1A. The protospacer adjacent motif (PAM) sequences are highlighted in purple and the sequences targeted by sgRNAs are underlined. The nucleotides altered at each target site are indicated in red. The codons for the modified amino acids are marked by dashes on the top. Four nucleotide changes were made in the *fis-2* gene and in the *ubr-1* gene, respectively, to generate a Hind III site (shaded in gray), resulting in a N49K missense mutation and a K50ochre nonsense mutation in the *fis-2* gene **(E)** and a silent mutation at Ala79 (GCA to GCT) and a M80ochre nonsense mutation in the *ubr-1* gene **(F)**.The red dashes (-) depict the deleted nucleotides. The green insertion marker (^) indicates the position of the inserted nucleotides or sequence. The numbers of deleted (-n) or/and inserted (+n) nucleotides are listed to the right of each sequence. The number in the parenthesis indicates the number of independently edited animals with the edited sequence shown on the left.

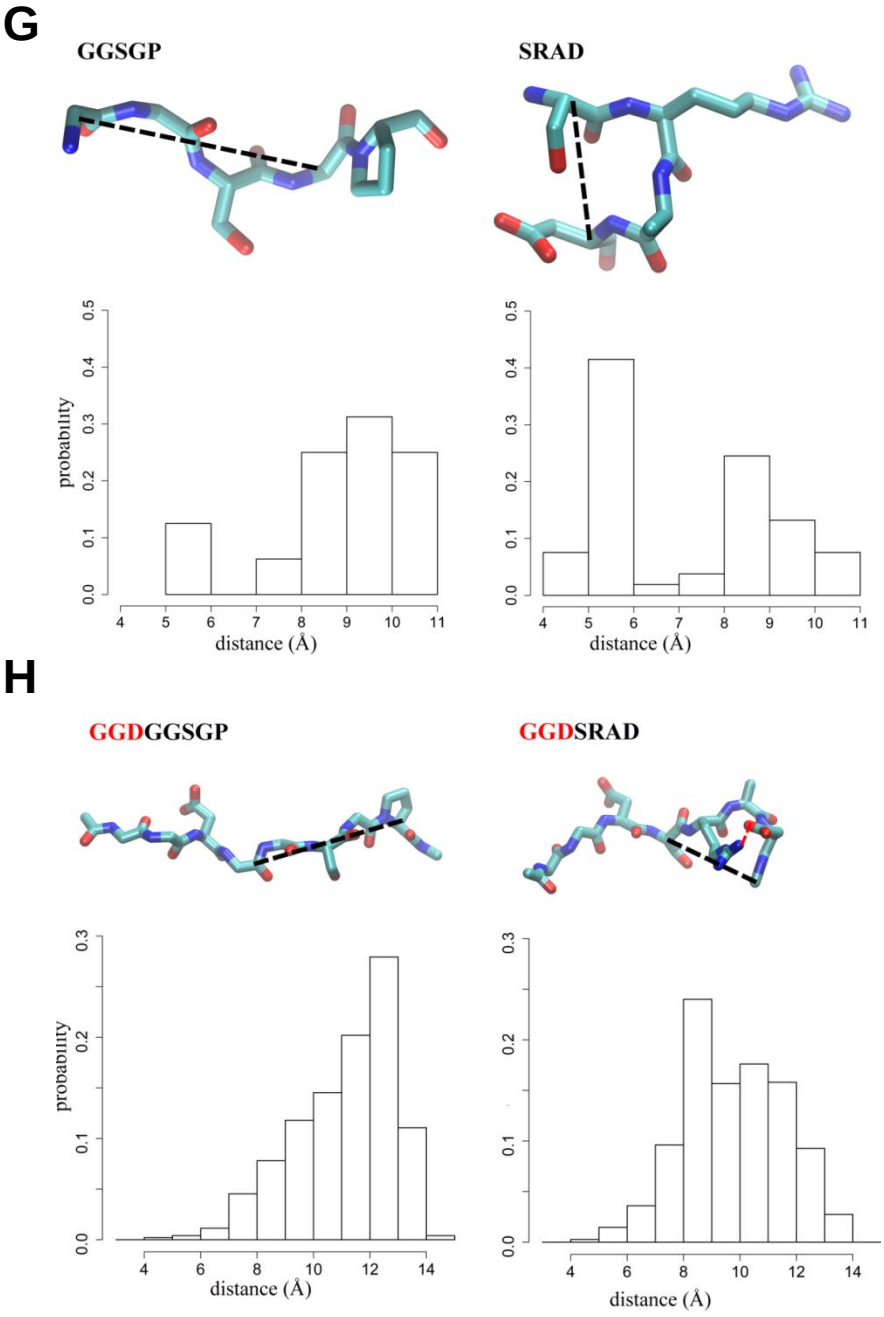

Supplementary information, Figure S2 A structurally optimized sgRNA$^{(F+E)}$ enhances the editing efficiency of Cas9 II and structural modeling of Cas9 I and Cas9 II. **(G)** The representative structures are taken from the crystal structures with PDB IDs of 2D9B and 1H6K, respectively. The EED is defined as the distance between the first and the fourth residues in the linkers, as indicated by the dashed black lines in the representative structures. **(H)** The representative structures for GGDGGSGP and GGDSRAD obtained from MD simulations on these two peptide fragments, respectively. The EED is calculated as the distance between the first and the fifth residues of GGSGP linker or between the first residue of the SRAD linker and the C terminal blocker of SRAD, as indicated by the dashed black lines in the representative structures. The dashed red line represents the electrostatic interaction between the Arg residue and the Asp residue in the SRAD linker. The probability distribution for EED is shown in histograms **(G, H)**.

I

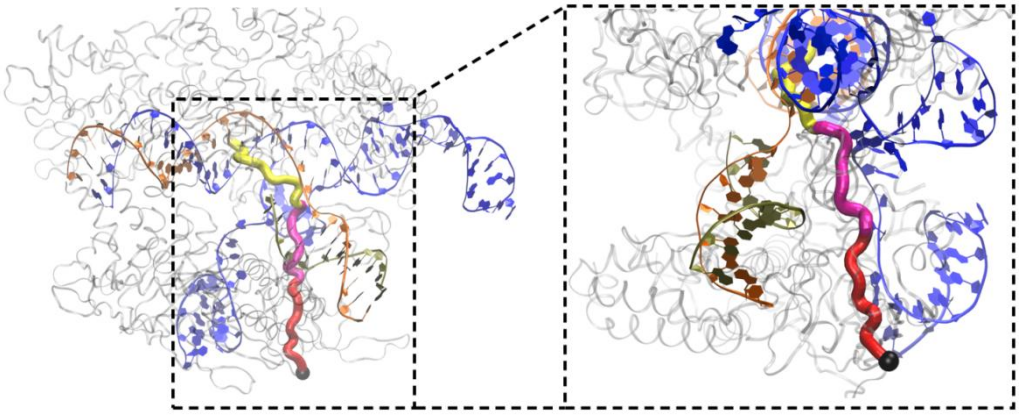

J

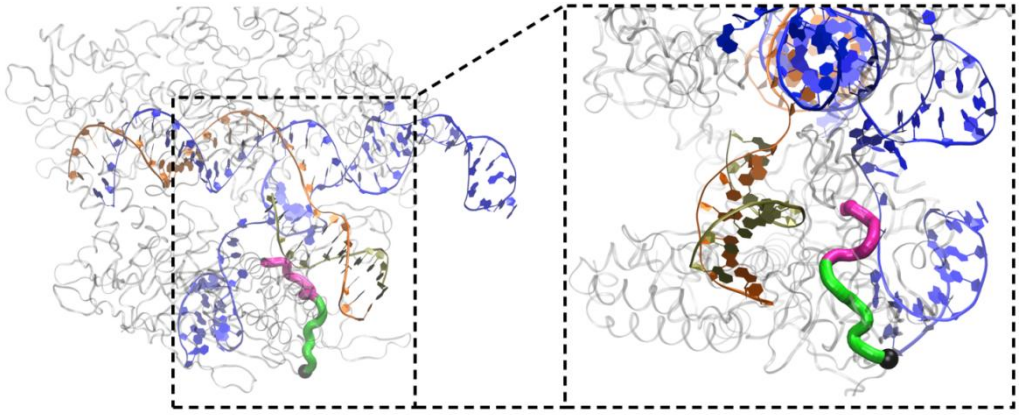

Supplementary information, Figure S2 A structurally optimized sgRNA$^{(F+E)}$ enhances the editing efficiency of Cas9 II and structural modeling of Cas9 I and Cas9 II. **(I, J)** The modeled structures of Cas9 II **(I)** and Cas9 I **(J)** (both from residue 3 to 1366 in the Cas9 portion) in complex with a sgRNA and a partial duplex DNA are shown using the New Ribbons representation in a silver and transparent mode. The structures of GGSGP (**I**) or SRAD (**J**), NLS and HA are shown using Ribbons representation in the color of red (GGDGGSGP), green (GGDSRAD), magenta (NLS) and yellow (HA), respectively. The sgRNA, target DNA and non-target DNA strands are shown using the New Ribbons representation and colored in blue, orange and tan, respectively. The Cα atoms of Gly1366 are presented as black spheres. The right panels in I and J are enlarged images of the boxed areas, which are also rotated 90 degree to show more clearly the interaction between the C-terminal tag of Cas9 and nucleic acids.

K

L

***drp-1*^{D118A}**

Cas9	Cas9 II	Cas9 XII	Cas9 XIII	Cas9 XIV
Knock-ins/Benomyl^{R} F1	50% (96/192)	32% (61/192)	13% (25/192)	4% (8/192)
Precise knock-ins/Sequenced	100% (21/21)	95% (18/19)	94% (17/18)	88% (7/8)
Normalized precise knock-ins/Benomyl^{R} F1	50% (96/192)	30% (58/192)	12% (24/192)	4% (7/192)
Homozygous knock-ins/Benomyl^{R} F1	3% (6/192)	1.6% (3/192)	1% (2/192)	0% (0/192)
Precise homozygous knock-ins/Benomyl^{R} F1	3% (6/192)	1.6% (3/192)	1% (2/192)	0% (0/192)

M

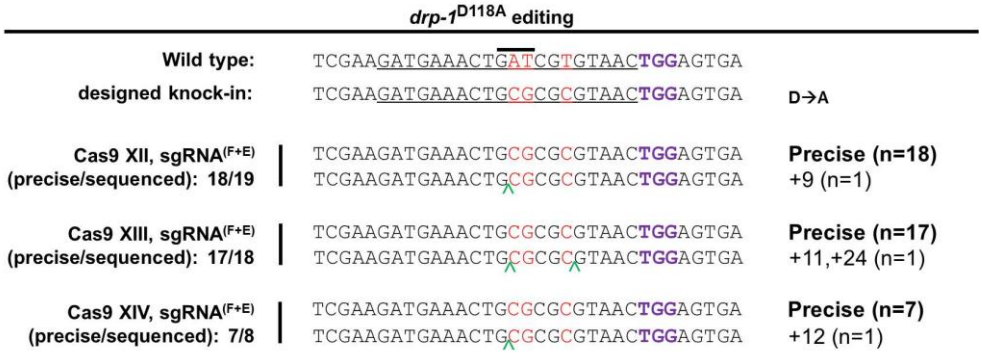

Supplementary information, Figure S2 A structurally optimized sgRNA$^{(F+E)}$ enhances the editing efficiency of Cas9 II and structural modeling of Cas9 I and Cas9 II. **(K)** A schematic diagram of Cas9 proteins with wild type and mutated HA tags. The black boxes depict the Cas9-coding exons and the blue lines depict the introns. The red boxes depict the GGSGP linker, the purple boxes depict SV40 NLS, and the yellow boxes depict wild type or modified HA tags, with the substituted amino acids highlighted in blue. **(L)** Comparison of gene editing efficiencies at the *drp-1*^{D118A} position by four different Cas9 proteins shown in K. A co-CRISPR method was used to enrich F1 edited animals at the target site. The *ben-1*^{153} sgRNA was used as a co-CRISPR driver. The number of knock-ins, homozygous knock-ins and precise homozygous knock-ins from the number of benomyl-resistant (benomyl^{R}) F1 animals isolated and the number of precise knock-ins from the number of knock-in animals sequenced are shown, respectively. The normalized percentage of precise knock-ins identified from the benomyl^{R} F1 animals screened is also shown. **(M)** Sequences of wild type animals and different Cas9-edited (Cas9 XII, Cas9 XIII and Cas9 XIV) animals around the *drp-1*^{D118A} position are shown as described in supplementary information, Figure S2B.

Supplementary Information, Table S1A List of oligonucleotide repair templates used in this study.

Oligo name	Sequence 5'-3'
***ben-1*^{22} oligo**	TCATATAACTTCAAAAAGAACTTGGAAAAAATGAGAGAAATT GTTCACGTTTAAGCCGGACAATGTGGTAATCAAATCGGAGCCA AGTTCTGGGAAGTGAT
***ben-1*^{153} oligo (±50nt)**	ACTTATAAGGGAGAAAGTGATTTGCAGTTGGAAAGAATCAAT GTCTACTAGAATGAGGCTAATGGTGAGAAATTTAGCTTTTTTA TTCGATTTTCAGATTC
***ben-1*^{1340} oligo**	TTCAGCCTCTTTTCGAACTACGTCGAGCACATTATCGACAAGTT CGGCTCATTCGGTGTAGTGACCCTTGGCCCAGTTGTTTCCGGCT CCGGATTGTCCGA
***ben-1*^{1499} oligo**	AATTAATCCAACCTTTGGCGACGGAACAACCGAGAAAGAACT CATAATTCAATCTGGATACTCTTCACGGATTTTCGAAATGAGA AGAGTTCCCATTCCAG
***drp-1* oligo**	TCGATGCCGTGCGAAAAGAAATCGAAGATGAAACTGCGCGCG TAACTGGAGTGAATAAAGGAATCTCTCTTCTTCC
***flag::ced-9* oligo**	TCTAGAATGTATATTATGATTATGAAAACGAATAAAAATTTTA GATGGACTACAAGGACGACGATGACAAGACACGCTGCACGGC GGACAACTCGCTGACGAATCCGGCGTATCGGCG
***fis-2* oligo**	GTCGACTTTTGCCTTTGCACATGCCATGATTGGATCCAAGCTTT AACTGGACGTGAAGGAGGGAATCGTGTGTCTTGAGAGTGA
***ubr-1* oligo**	CTAGACGTTCGGAACACAAAGAGCACACTGGAAGCTTAAAAT GGCATTGCCGGAGTTGATCCTGCAAGACGGGG
***ben-1*^{153} oligo (±25nt)**	AGTTGGAAAGAATCAATGTCTACTAGAATGAGGCTAATGGTGA GAAATTTA
***ben-1*^{153} oligo (±20nt)**	GAAAGAATCAATGTCTACTAGAATGAGGCTAATGGTGAGAA
***ben-1*^{153} oligo (±15nt)**	AATCAATGTCTACTAGAATGAGGCTAATGGT
***ben-1*^{153} oligo (±10nt)**	ATGTCTACTAGAATGAGGCTA
***ben-1*^{136} oligo**	ACTTATAAGGGAGAAAGTGATTTGCAGTTGGAATGAATCAATG TCTACTATAATGAGGCTAATGGTGAGAAATTTAGCTTTTTTATT CGATTTTCAGATTC
***ben-1*^{127} oligo**	AACTTATAAGGGAGAAAGTGATTTGTAGTTGGAAAGAATCAAT GTCTACTATAATGAGGCTAATGGTGAGAAATTTAGCTTTTTTAT TCGATTTTCAGATTC
***ben-1*^{115} oligo**	CCAGCCTGATGGAACTTATAAGGGATAAAGTGATTTGCAGTTG GAAAGAATCAATGTCTACTATAATGAGGCTAATGGTGAGAAAT TTAGCTTTTTTATTCGATTTTCAGATTC

Supplementary Information, Table S1B List of primers used in this study.

Usage	Primer	Sequence (5'-3')
Genotyping	*ben-1* F1	CCCTGGCTAGTTCAAACGAAGAG
	ben-1 R1	CCCATAGGTTCCCGTATGTC
	ben-1 F2	TGCGCATTCGCGCTCTATAGCAACC
	ben-1 R2	CGTCCACGGAACATTGCAGCTACAG
	drp-1 F	TCCACAGATTGTAGTCGTCG
	drp-1 R	CTTTCAGTGCAGGAAGACAG
	ced-9 F	TTTGCCGTTCGATTTCACCG
	ced-9 R	TGTGCATTTCCAACCGTCCG
	fis-2 F	ACTATTCTCGAGGAACGGAC
	fis-2 R	ACCCGTTCACTTTTGTTCCG
	ubr-1 F	TACGCCAGCTGCTGCTCAAG
	ubr-1 R	CCGTCAAATATTGCTGTGCC
Allele-specific primers	*ced-9* flag F	TTGTTTTGAAACGCACCGCC
	ced-9 flag R	CATCGTCGTCCTTGTAGTCC
	ced-9 N2 F	CGAATAAAAATTTTAGATGACACGC
	ced-9 N2 R	GTGTTCCTTCCAGTTGTTGC

To confirm that precise knock-ins occurred at the targeted sites in edited animals, genomic DNA spanning each sgRNA target site was PCR amplified using "genotyping" primers and subjected to sequencing analysis. The *ben-1* F1/R1 primer pair was used to amplify the genomic DNA spanning the *ben-1*^{22} and *ben-1*^{153} positions. The *ben-1* F2/R2 primer pair was used to amplify the genomic DNA spanning *ben-1*^{1340}, *ben-1*^{1499} sgRNA target sites. *drp-1* F/R, *ced-9* F/R, *fis-2* F/R and *ubr-1* F/R primer pairs were used to amplify the genomic DNA spanning the *drp-1*, *ced-9*, *fis-2* and *ubr-1* sgRNA target sites, respectively. For *drp-1*, *fis-2* and *ubr-1* editing experiments, the same PCR products were digested with restriction enzymes to identify the knock-in animals. In the *flag::ced-9* editing experiments, we used allele-specific primers to identify *flag::ced-9* knock-in animals (*ced-9* flag F/R) from benomyl^{R} F1 animals and homozygous F2 animals with knock-ins (*ced-9* flag F/R and *ced-9* N2 F/R).